FULL PULSE ANALYSIS OF X-BAND HIGH-GRADIENT TEST DATA TAKEN AT Nextef2

Tetsuo Abe*, Mitsuo Akemoto, Yasuo Higashi, Toshiyasu Higo, Shuji Matsumoto,
High Energy Accelerator Research Organization (KEK), Tsukuba, Japan
Daisuke Satoh,
National Institute of Advanced Industrial Science and Technology (AIST), Tsukuba, Japan
Takuya Kudou, Shiro Kusano,
Mitsubishi Electric System & Service Co., Ltd., Tsukuba, Japan

Abstract

At an X-band (11.4 GHz) high-power test facility at KEK, Nextef2, we have been conducting high-gradient tests of various normal-conducting accelerating structures. The practical high-gradient performance of the structures is mainly determined by the frequency of breakdowns caused by vacuum arcs. At the moment of breakdown, in addition to large on-axis currents from vacuum arcs, characteristic waveforms associated with RF reflection appear. In our previous high-gradient tests, only the data from the final RF pulse or the last ten pulses prior to breakdown were stored and analyzed. However, the occurrence of breakdown is the result of cumulative pulse application over many cycles, so that it may be possible to observe precursors to breakdown at an earlier stage. Furthermore, breakdown is not a binary phenomenon; an intermediate state, which could be a precursor, might also be observed. Based on the above, we have constructed a system that can store and analyze all RF pulse information with a repetition rate of 50 Hz by introducing a digitizer in order to deepen our understanding of the breakdown phenomena. In this paper, we report on the system and results of the initial analysis of all pulses obtained during high-power RF conditioning of an X-band test cavity.

INTRODUCTION

X-band (9 to 12 GHz) linear accelerators are now being developed for various applications including medical, industrial, and academic disciplines around the world (e.g. see [1]). Due to the compactness enabled by a high frequency, the accelerating gradients or accelerating fields are mostly much higher than those of widely used C-band (around 5.7 GHz) or S-band (around 2.8 GHz) accelerating structures. Therefore, it is important to understand vacuum breakdown (BD) phenomena caused by vacuum arcs that are triggered by a high surface field in an accelerating structure. The most common tool to detect BD is a Faraday cup (FC) located on-axis upstream or downstream to measure electron currents originated from vacuum arcs. Another method for standing-wave cavities is to measure characteristic RF-pulse waveforms associated with RF reflection from the cavity, as studied in [2]. However, usually, only the data from the final pulse or the last several pulses prior to BD were stored and analyzed. Because the occurrence of BD is the result of cumulative pulse application over many cycles, it may be possible to observe precursors to BD at an earlier stage. Furthermore, BD is not a binary phenomenon; an intermediate state, which could be a precursor, might also be observed. Based on the above, we have constructed a system that can store and analyze all RF-pulse information with a repetition rate of 50 Hz by introducing a digitizer in order to deepen our understanding of the BD phenomena. In this paper, we report on the system and results of the initial analysis of all pulses obtained during high-power RF conditioning of an X-band test cavity explained in the next section.

Abbreviations and a symbol used in this paper are listed in Table 1 in the appendix.

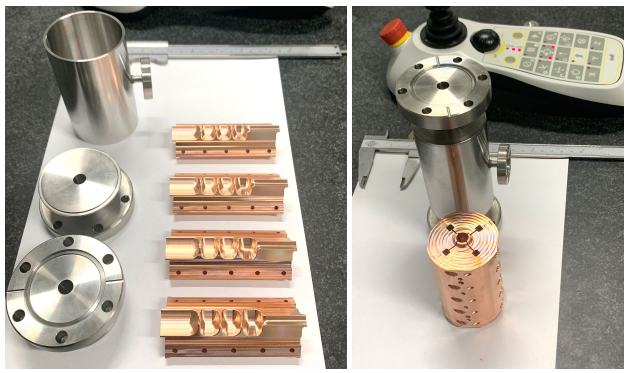

Figure 1: X-band single-cell test cavity fabricated from longitudinally-split four quadrants made of copper, which were clamped and installed into a cylindrical vacuum vessel made of SUS [3].

TEST CAVITY

The test cavity in this study is shown in Fig. 1, which was designed and fabricated by INFN-LNF in Italy and SLAC in USA. The cavity consists of three cells, an input matching cell, an end cell, and a central test cell. The cavity was designed so that the field strength in the central test cell is much higher than those in the input matching and end cells. The details of the cavity are described in [3]. Via the US-Japan cooperative program, the cavity was sent to KEK, and installed into an X-band (11.4 GHz) high-power test stand: Nextef2 [4], as shown in Fig. 2. The cavity was high-power RF conditioned up to around 4 MW with an input RF pulse

* tetsuo.abe@kek.jp

length of 100 ns, corresponding to an accelerating gradient in the central test cell (E_{acc}) of approximately 60 MV/m. The details of the high-power test were shown in [5]. Immediately prior to the high-power test, we installed a digitizer system to Nextef2 so that we can store all waveforms of RF pulses to obtain more understanding and insights, that is a theme of this paper.

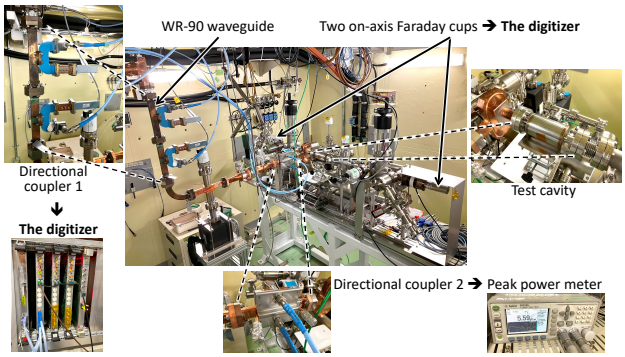

Figure 2: Setup of the high-gradient test in Nextef2. There are two sets of directional couplers, one of which is connected to the digitizer, and the other is connected to a peak power meter. Two FCs are located on-axis upstream and downstream to measure currents from vacuum arcs.

DIGITIZER

The digitizer system includes three flash ADC (FADC) boards of SIS3305 from Struck Innovative Systeme, each of which has four input channels, in addition to a CPU board of MVME55006E-0163, which are all installed in a VME rack of LHC9867-10BP, as shown in Fig. 3(a). In the CPU, vxWorks6.8.3 and EPICS [6] Base R3.14.12 are installed. EPICS IOC is running in the environment to collect measurements in the FADC boards through a VME bus. Finally, measurements stored as EPICS records in the digitizer are sent to Archiver Appliance [7] through a private GbE network.

The maximum sampling rate and number of sampling points using twelve (= 4 × 3) input channels simultaneously are 1.25 GHz and 1000, respectively, leading to a time span of 800 ns which is much longer than the maximum high-power RF-pulse length of 400 ns available at Nextef2. In this study, we used only one FADC board for the RF input to and reflection from the cavity, upstream and downstream FCs. The data size per one-month continuous operation with a maximum repetition rate of 50 Hz is approximately 1 TB, which is much smaller than the currently available storage size in our server computer (> 20 TB). We have confirmed no missing pulse in the archived data taken for one day which includes approximately four million pulses.

NEW QUANTITIES

In most of high-power tests of X-band high-gradient accelerating structures, only FCs are used to detect BD. However,

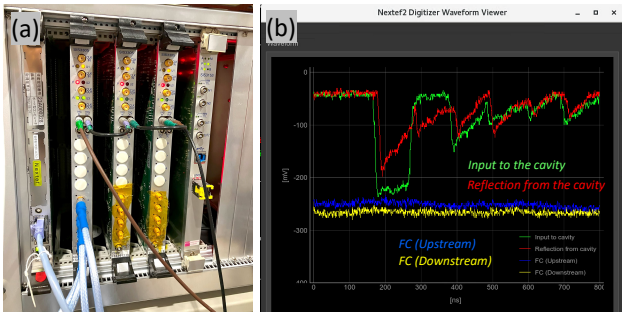

Figure 3: (a) Digitizer boards installed in the VME rack. (b) Waveforms of data taken with the digitizer, where the green and red lines indicate the RF input to and reflection from the cavity, respectively, and the blue and yellow lines indicate upstream and downstream FC signals, respectively. It should be mentioned that there is no high-power circulator between the klystron and test cavity, so that RF pulses reflected at the test cavity come back after round trip of approximately 200 ns (corresponding to the second peak in the input pulse).

reflection RF waveforms might be important for standing-wave cavities [2]. Therefore, we here define new quantities to effectively detect abnormal RF-pulse waveforms in big data as follows:

$$\bar{t} \stackrel{\text{def}}{=} \frac{1}{V}\sum_{i}^{win} |v_i|\, t_i\,, \tag{1}$$

$$\check{t} \stackrel{\text{def}}{=} t_m \text{ for } \sum_{i=1}^{m-1} |v_i| < \frac{V}{2} \text{ and } \sum_{i=1}^{m} |v_i| > \frac{V}{2}\,, \tag{2}$$

$$\sigma \stackrel{\text{def}}{=} \sqrt{\frac{1}{V}\sum_{i}^{win} |v_i|\, t_i^2 - \bar{t}^2}\,, \tag{3}$$

where t_i indicates the i-th time of the sampling in the digitizer, v_i indicates a voltage detected at the time of t_i, V is an integrated absolute voltage: $V = \sum_i^{win} |v_i|$, and $\sum_i^{win}$ indicates summation over the time window defined in Fig. 4(a) with white vertical lines, which includes only the first pulse input to the cavity, excluding the second pulse after round trip. The above time statistic quantities for each RF pulse, $\bar{t}$, $\check{t}$, and σ mean an average time, median time, and standard deviation in time of each pulse in the time window, respectively. Examples of the new quantities are also shown in Fig. 4. Figure 4(b) and (c) indicate height and average (or area) of each pulse, respectively, as a function of the pulse number (or time) for 3000 consecutive RF pulses taken for one minute with a repetition rate of 50 Hz. Figure 4(d), (e), and (f) indicate $\bar{t}$, $\check{t}$, and σ ,respectively, for the same time period. As seen in Fig. 4, $\bar{t}$, $\check{t}$, and σ are RF-power independent. This is the most useful and convenient characteristic, particularly for high-power RF conditioning where the RF power is frequently changed over a wide range.

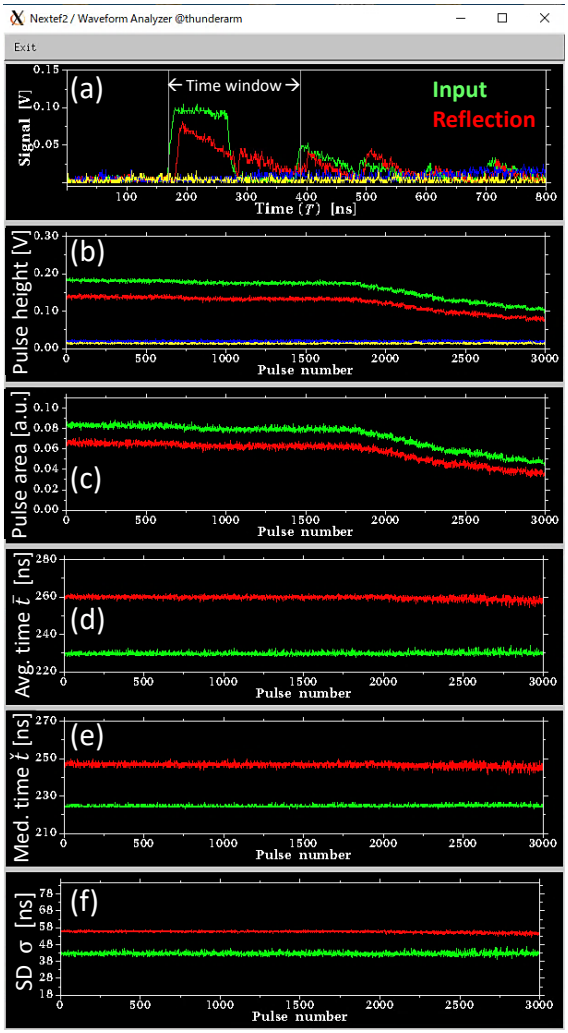

Figure 4: (a) Definition of the time window used for the summation $\sum_i^{win}$. (b) to (f) Examples of histories of the new time statistic quantities for each RF pulse.

DATA ANALYSIS

Examples of BD Detections

In order to effectively collect data including BD candidate events, we performed the high-power test without stopping high-power RF feeding even when BD was detected by an abnormal reflection waveform or a FC unless any hardware interlock worked.

Figure 5 shows data for 20 seconds including 1000 pulses with $E_{acc} \approx 60$ MV/m. There are many BDs for approximately two seconds with 100 pulses; however, not consecutive, but intermittent. BD pulses are characterized by a significantly earlier $\bar{t}$ and/or $\check{t}$ because the microwave energy in the cavity is eaten by vacuum arcing of BD, leading to a lower reflection level or almost no reflection after BD starts. The vacuum pressure measured near the cavity increased over a software threshold of 1×10^{-4} Pa, so that the RF power was automatically stepped down by computer control, then the BD burst subsided. During the BD burst, there were significant signals from the downstream FC as shown in the top figure of Fig. 5(a) with yellow lines. This event is as we understand and expect.

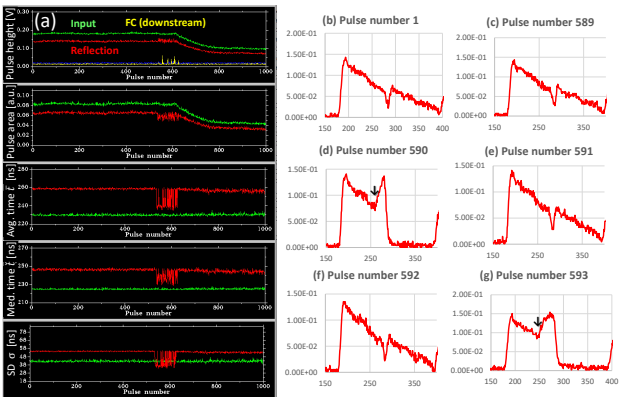

Figure 5: Example of the digitizer data: 20 second data with 1000 pulses taken from 20:56:20 to 20:56:40 on 2025/03/09, including an intermittent BD burst. (a) Histories of the new quantities for each pulse. (b), (c), (e), (f) are normal reflection pulses. The vertical arrows in (d) and (g) indicate an expected timing when BD started.

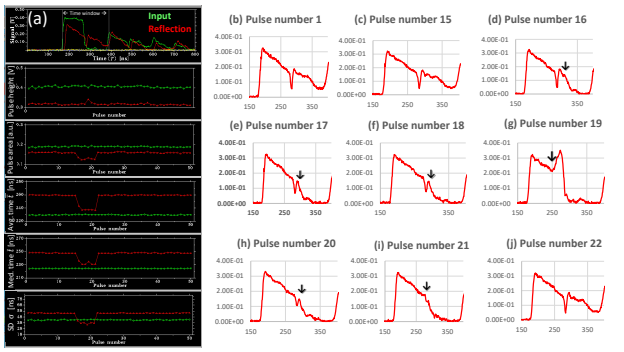

Figure 6: Example of the digitizer data: six consecutive BDs taken at 20:55:48 on 2025/02/25 for one second with 50 pulses. The vertical arrows indicate an expected timing when BD started.

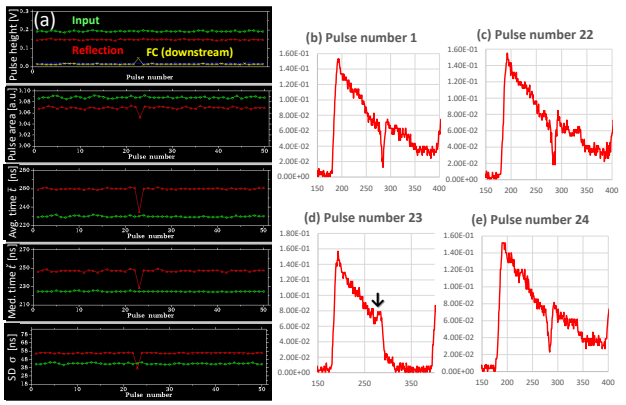

Figure 7: Example of the digitizer data: there was only a single BD observed at 13:58:04 on 2025/03/16 together with a significant signal in the downstream FC. The vertical arrow indicates an expected timing when BD started.

Figure 6 shows data for one second including 50 pulses with $E_{acc} \approx 40$ MV/m. There were six successive BD pulses with a vacuum pressure rise close to 1×10^{-4} Pa below the software threshold. It is remarkable that the reflection waveform recovered to normal without decreasing the RF power, which is unexpected because the cavity was conditioned during such a short time only with six pulses. It should be also noted that only a small single spike was observed in the trend of the reflection-pulse height during the six successive BDs. The reason is that normal reflection pulses have a large transient peak at the start of each input pulse, that overshadows BD information.

Figure 7 is a more extreme example, showing a single momentary BD with $E_{acc} \approx 60$ MV/m, where the input RF power was maintained at the constant level during the one second period as shown in Fig. 7(a). The vacuum pressure rise was much smaller than those of the above two examples, from approximately 3×10^{-6} Pa up to 1×10^{-5} Pa. If we had stopped the RF-power feeding by the single BD pulse, we would have wasted time of high-power operation.

Distributions and Correlations

Figure 8 shows distributions of $\bar{t}$, $\check{t}$, and σ of reflection pulses in data taken during three-day continuous operation. In Fig. 8(a), normal and BD pulses are well separated, meaning that $\bar{t}$ is a good quantity to detect BD. On the other hand, normal and BD pulses are not separated in Fig. 8(b), so that $\check{t}$ is not useful to detect BD. Similarly, Fig. 8(c) says that σ is also a good quantity to detect BD.

Figure 9 shows correlations of $\bar{t}$ with other quantities. In Fig. 9(a), a clear separation is seen between the normal and BD pulses together with a clear correlation that BD pulses have an earlier timing and a narrower shape, that is consistent with our understanding of BD pulses. In addition, it seems that there is a structure in the group of BD pulses with at least two subgroups although the amount of experimental data is not sufficient to draw a conclusion. From Fig. 9(b), it is found that reflection waveforms are much more sensitive to BD than FC signals since BD pulses have a peak near zero in the FC signal. Therefore, relying solely on FCs is not sufficient for highly-sensitive BD detection.

The subgroup indicated with a horizontal arrow in Fig. 9(b) is under investigation.

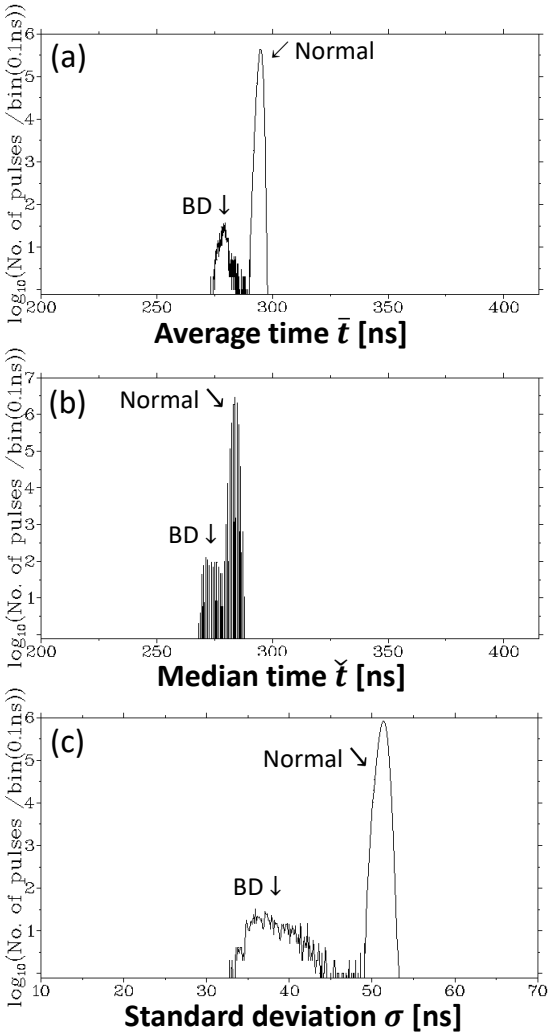

Figure 8: Distributions of the time statistic quantities for 8 034 112 reflection pulses taken during the three-day continuous operation, where only pulses with RF powers input to the cavity higher than 1.5 MW ($E_{acc} \gtrsim 36$ MV/m) are included in this figure to exclude data with low signals. (a) Average time $\bar{t}$. (b) Median time $\check{t}$. (c) Standard deviation σ. The vertical axes indicate number of reflection pulses in log scale.

SUMMARY AND CONCLUSIONS

We have installed the digitizer system in Nextef2 to store and analyze all RF pulses during high-gradient tests of X-band normal-conducting accelerating structures. In order to effectively detect BD, we have defined new time statistic quantities, $\bar{t}$, $\check{t}$, and σ, which enables us to detect BD using only a single quantity ($\bar{t}$ or σ). Normal pulses have the same value for each quantity even if RF-power changes unless the input pulse shape is changed.

From the initial analysis using the digitizer and the new quantities, we have obtained the following findings: (A) Even when some BDs occurred, natural recovery was observed without decreasing the RF power; (B) Reflection waveforms are much more sensitive to BD than on-axis FCs. The above finding (A) suggests that high-power operation of standing-wave accelerating structures should not be stopped by a single BD pulse. One possible improvement could be to adopt a series of BD pulses within a certain time instead of a single BD pulse. The above finding (B) is important because BD rates of accelerating structures measured in high-power tests could be underestimated if BD is detected only with FCs.

It should be noted that the above conclusions are made only for the test cavity in [3]. In the future, we will continue to use the digitizer and the new quantities storing and analyzing all RF pulses for other accelerating structures in

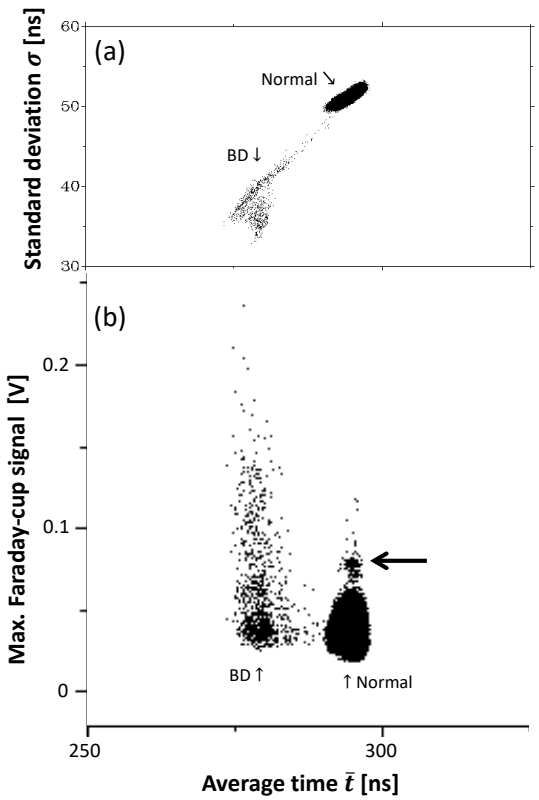

Figure 9: Correlations of $\bar{t}$ with other quantities for 8 034 112 reflection pulses, where the used data is the same as in Fig. 8. The vertical axis of (b) indicates the maximum signal level between the upstream and downstream FCs.

order to see if the conclusions are universal or not. The new quantities have already been used in data analysis of a high-gradient test for a dielectric-assist structure [8].

APPENDIX

Table 1 lists the abbreviations and symbol used in this paper.

Table 1: Abbreviations and Symbol Used in This Paper

Abbreviation	Full letters
ADC	Analog-to-digital converter
BD	Breakdown
CPU	Central processing unit
FC	Faraday cup
GbE	Gigabit ethernet
IOC	Input/output controller
Nextef	New X-band test facility
RF	Radio frequency
VME	Versa module eurocard
E_{acc}	Accelerating gradient

REFERENCES

[1] *16th Workshop on Breakdown Science and High Gradient Accelerator Technology (HG2025)*, https://indico.fnal.gov/event/65159/, 2025.

[2] T. Abe *et al.*, "High-Gradient Testing of Single-Cell Test Cavities at KEK / Nextef", in *Proceedings of the 13th Annual Meeting of Particle Accelerator Society of Japan, MOP015*, 2016. https://www.pasj.jp/web_publish/pasj2016/proceedings/PDF/MOP0/MOP015.pdf

[3] V. Dolgashev, L. Faillace, M. Migliorati, and B. Spataro, "Investigations on the multiple-sector hard-copper x-band accelerating structures", *Nuclear Instruments and Methods in Physics Research Section A: Accelerators, Spectrometers, Detectors and Associated Equipment*, vol. 1063, p. 169 272, 2024. https://www.sciencedirect.com/science/article/pii/S0168900224001980

[4] T. Abe *et al.*, "Nextef2: Reborn X-Band High-Gradient Test Stand at KEK", in *Proceedings of the 19th Annual Meeting of Particle Accelerator Society of Japan, TUP049*, 2022. https://www.pasj.jp/web_publish/pasj2022/proceedings/PDF/TUP0/TUP049.pdf

[5] T. Abe, "High-Power Testing of X-Band Multiple-Sector Single-Cell Test Cavities at Nextef2", in *the 16th Workshop on Breakdown Science and High Gradient Accelerator Technology (HG2025)*, 2025. https://indico.fnal.gov/event/65159/contributions/311812/

[6] *Experimental Physics and Industrial Control System*. https://epics.anl.gov/

[7] I. Satake *et al.*, "Operation Status of Archiver Appliance in KEK Electron/Positron Injector Linac", in *Proceedings of the 17th Annual Meeting of Particle Accelerator Society of Japan, FRPP25*, 2020. https://www.pasj.jp/web_publish/pasj2020/proceedings/PDF/FRPP/FRPP25.pdf

[8] D. Satoh *et al.*, "Research toward high gradient X-band dielectric assist accelerating structures", in *Proceedings of the 22nd Annual Meeting of Particle Accelerator Society of Japan, FRP050*, 2025.